Advances in Nano Research, *Vol. 11, No. 1 (2021) 55-71*
https://doi.org/10.12989/anr.2021.11.1.055

Mechanical analysis of bi-functionally graded sandwich nanobeams

Doan Trac Luat, Do Van Thom, Tran Trung Thanh, Phung Van Minh, Tran Van Ke and Pham Van Vinh*

Department of Solid Mechanics, Le Quy Don Technical University, 236 Hoang Quoc Viet, North Tu Liem, Hanoi, Vietnam

(*Received December 14, 2020, Revised April 21, 2021, Accepted May 8, 2021*)

Abstract. In this study, the bending, free vibration and buckling analysis of a novel bi-functionally graded sandwich nanobeam are investigated for the first time via a nonlocal refined simple shear deformation theory. The novel sandwich beam consists of one ceramic core and two different functionally graded face sheets, which has a significant potential application in various fields of practical engineering and industry. The Eringen's nonlocal elastic theory has been used in cooperation with a refined simple shear deformation theory as well as Hamilton's principle to derive the equations of motion. Closed-form solution based on Navier's technique is used to solve the equations of motion of simply supported nanobeams. The present numerical results are compared with the available solutions to demonstrate the accuracy of the present theory. The influence of some parameters such as the slender ratio, the power-law index, the skin-core-skin thicknesses and the small-scale parameter on the bending, free vibration and buckling behavior of bi-functionally graded sandwich nanobeams are carried out carefully.

Keywords: bi-functionally graded sandwich beams; nanobeams; nonlocal theory; refined simple shear deformation theory; sandwich beams

1. Introduction

Nowadays, the use of the multi-layer structures such as laminated composites, sandwich structures is increasing rapidly especially in some special fields of nuclear energy, aerospace and aeronautics science, defence technology, medical field, etc. However, the disadvantage of the traditional layered structures is that the material properties vary discontinuously through the thickness of the structures, so the delamination damage may occur at the contact surface. To overcome this phenomenon, the FGM sandwich structures with the material properties vary continuously through the thickness of the structures have been introduced and used widely (Bakoura *et al*. 2021, Hadj *et al*. 2019, Zine *et al*. 2020, Vinh 2021). Therefore, many scientists have been focused on the investigation on the mechanical, thermal behavior of these structures. It is obvious that the functionally graded sandwich plates and beams are the most important structures which are widely used in the engineering and industry (Boussoula *et al*. 2020, Chikr *et al*. 2020, Menasria *et al*. 2020, Rabhi *et al*. 2020). So, the study of the static bending, buckling and free vibration of the functionally graded sandwich (FGSW) beams is necessary. The FGSW beams can be modelling via classical beam theory (CBT), first-order shear deformation theory (FSDT), higher-order shear deformation theories (HSDTs) or normal deformation (quasi-3D) theories. Apetre *et al*. (2008) used a HSDT incorporation with Fourier-Galerkin method to modelling and analyze the behavior of FGSW beams. Nguyen and Nguyen (2015) developed a new HSDT to analyze the bending, buckling and free vibration of FGSW beams with homogeneous hardcore and softcore. Nguyen *et al*. (2015) studied the vibration and buckling of FGSW beams using new HSDT with new hyperbolic distribution function. A new refined hyperbolic HSDT had been developed by Riadh *et al*. (2015) to investigate the vibration and buckling of FGSW beams under various boundary conditions. Vo *et al*. (2014) developed a finite element model based on a refined HSDT for analysis of FGSW beams. Li *et al*. (2019) developed an HSDT mixed beam element to investigate the bending of the FGSW beams. A quasi-3D theory has been introduced by Vo *et al*. (2015a, 2015b) to study the bending, free vibration and buckling behavior of the FGSW beams. Nguyen *et al*. (2016) used a quasi-3D theory to develop an analytical solution for buckling and free vibration analysis of the FGSW beams. Osofero *et al*. (2015) studied the vibration and buckling behavior of the FGSW beams using various quasi-3D theories. Karamanlı (2017) investigated the bending behavior of the two-directional FGSW beam by using a quasi-3D theory. Yarasca *et al*. (2016) developed a Hermite-Lagrangian finite element to study the FGSW beams. The free vibration and stability of the FGSW beams had been studied by Tossapanon and Wattanasakulpong (2016). The vibration and dynamic response of the FGSW beams have been investigated by Şimşek and Al-shujairi (2017), and Songsuwan *et al*. (2018). The state space approach had been used to analyze the free vibration of the FGSW beams by Trinh *et al*. (2016).

Recently, micro/nanostructures have been investigated and applied in many fields of engineering. The behavior of these structures is completely different in comparison with the usual structures due to the small-scale effects of the micro and nanostructures. To investigate these structures,

*Corresponding author, M.Sc.,
E-mail: phamvanvinh@lqdtu.edu.vn

ISSN: 2287-237X (Print), 2287-2388 (Online)

many theories have been introduced such as dynamic of molecular (DOM), couple stress theory (CST) and modified couple stress theory (MCST), strain gradient theory (SGT), nonlocal elastic theory (NET), nonlocal strain gradient theory (NSGT). Gao and Zhang (2015) developed a new beam model based on third-order shear deformation theory and MCST. Thai and Vo (2012) developed a nonlocal sinusoidal shear deformation theory (SSDT) to analyze static bending, free vibration and buckling behavior of nanobeams. Zemri *et al*. (2015) analyzed mechanical behavior of the FG nanobeams using a refined nonlocal shear deformation beam theory. Larbi *et al*. (2015) studied the bending of the FG nanobeams using nonlocal continuum model based on a normal shear deformation theory. The effect of the neutral surface on the bending and buckling of the FG nanobeams had been investigated by Mama *et al*. (2016). The free vibration of the FG nanobeams had been investigated by Hamed *et al*. (2016) via Euler-Bernoulli beam theory and NET. Balibaid *et al*. (2019) and Berghouti *et al*. (2019) investigated free vibration of FG nanoplates and porous nanobeams using two variables integral refined plate theory and NET. Bellal *et al*. (2020) used nonlocal four-unknown integral model to analyze buckling behavior of single-layered graphene sheet. Matouk *et al*. (2020) used an integral Timoshenko beam theory in combination with NET to analyze hygro-thermal vibration of P-FG and S-FG nanobeams. Bouafia *et al*. (2017) developed a nonlocal quasi-3D theory to analyze free flexural vibration of FG nanobeams. Boutaleb *et al*. (2019) analyzed dynamic response of FG nanoplates using a simple nonlocal quasi-3D theory. A nonlocal zeroth-order shear deformation theory had been developed by Bellifa *et al*. (2017) to analyze nonlinear post-buckling of nanobeams. Yang *et al*. (2018) analyzed nonlinear bending, buckling and vibration of bi-directional functionally graded nanobeams by using Euler-Bernoulli beam theory. Ahmed *et al*. (2018) studied buckling behavior of the FG nanobeams using a new quasi-3D theory in combination with NSGT. In this work, the variation of the length scale parameter is considered. Yang *et al*. (2019) used NSGT in combination with an HSDT based on the physical neutral surface to analyze the nonlinear thermal buckling of bi-directional FG nanobeams. Aria *et al*. (2019) established a finite element model based on the FSDT and NET to analyze the thermo-elastic behavior of FG nanobeams with porosity. A comprehensive study on the static bending, free vibration and buckling behavior of FG nanobeams had been carried out by Şimşek (2019), in which he used some closed-form solution based on Euler-Bernoulli and NSGT. Hana *et al*. (2019) investigated the nonlocal vibration of FG nanobeams with porosity. Aria and Friswell (2019) developed a strain-driven (nonlocal) finite element model based on the FSDT to examine the free vibration and buckling behavior of the FG nanobeams. Arefi and Zenkour (2016) established a simplified shear and normal deformations nonlocal theory to study the bending behavior of FG piezomagnetic sandwich nanobeams in the magnetic-thermo-electric environment. Zhang and Gao (2020) developed a new Bernoulli-Euler beam model based on a reformulated SGT. Liu *et al*. (2019) examined the nonlinear free vibration of geometrically imperfect FGSW nanobeams via NSGT. Bensaid *et al*. (2020) investigated the size-dependent free vibration and buckling behavior of sigmoid and power-law FGSW nanobeams via an HSDT and NET.

It can be seen that there is no study in the past working on the mechanical behavior of a bi-functionally graded sandwich (bi-FGSW) nanobeams which are made of two different FGM face sheets. These structures can be applied in many fields of engineering and industry where the structures always contact to the different environment on two surfaces. The rapid development of artificial intelligence and three-dimension printing technology can make the process of creating the bi-FGSW nanobeams easier. So, a comprehensive study on the mechanical behavior of the bi-FGSW nanobeams is very necessary, and it is the main aim of this study. In this study, the NET will be used to take into account the small-scale effects on the mechanical behavior of bi-FGSW nanobeams. The outlines of this study are as follows: section 2 gives the geometry and construction of bi-FGSW nanobeams and the theoretical formulation. The comparison study and main numerical results of the mechanical behavior of the bi-FGSW nanobeams are given in section 3. Section 4 gives some remarkable summaries, main distribution of the present work and some suggestions for future works.

2. Theoretical formulation

2.1 Bi-functionally graded sandwich nanobeams

In this study, a novel functionally graded sandwich nanobeam as shown in Fig. 1, which is called bi-functionally graded sandwich (bi-FGSW) nanobeam, is considered. The novel sandwich nanobeam consists of one homogeneous ceramic core and two different FGM face sheets which have similar ceramic component and have different metal components.

The volume fraction of the ceramic component of the bi-FGSW nanobeam is

$$\begin{cases} V_c^{\text{bottom}} = \left(\dfrac{z-z_0}{z_1-z_0}\right)^k & z_0 \le z \le z_1 \\ V_c^{\text{core}} = 1 & z_1 < z < z_2 \\ V_c^{\text{top}} = \left(\dfrac{z-z_3}{z_2-z_3}\right)^k & z_2 \le z \le z_3 \end{cases} \tag{1}$$

It can see clearly that the core layer of the sandwich beam is made of homogeneous ceramic, while the volume fraction of the ceramic component varies continuously through the thickness of two face sheets. The effective material properties through the thickness of the beam are obtained by the following formulae

$$\begin{aligned} E(z) &= E_m^{(i)} + (E_c - E_m^{(i)})V_c \\ \rho(z) &= \rho_m^{(i)} + (\rho_c - \rho_m^{(i)})V_c \\ \nu(z) &= \nu_m^{(i)} + (\nu_c - \nu_m^{(i)})V_c \end{aligned} \tag{2}$$

where E_c, ρ_c, ν_c denote Young's modulus, the mass

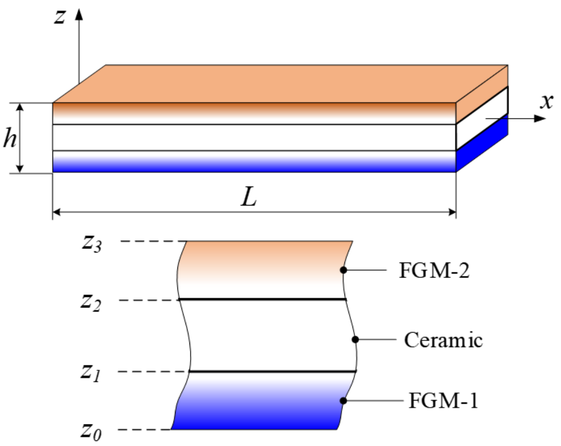

Fig. 1 The model of the bi-FGSW nanobeams

Table 1 The material properties of individual materials

Materials	Young's modulus (GPa)	Mass density (kg/m^3)	Poison's ratio
Ti-6Al-4V	66.2	4420	1/3
SUS304	207	8166	0.3
Si_3N_4	323	3170	0.3

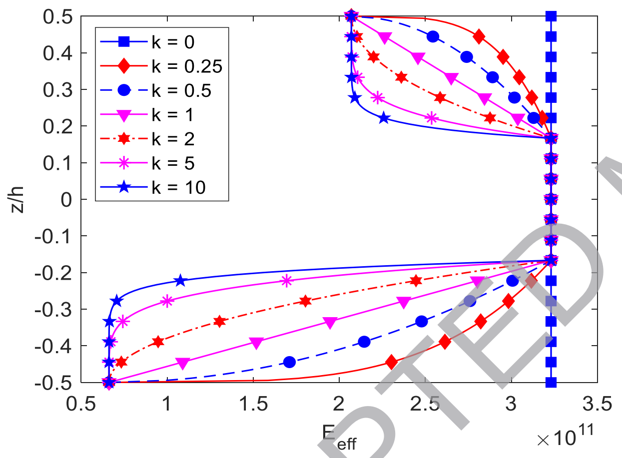

(a)

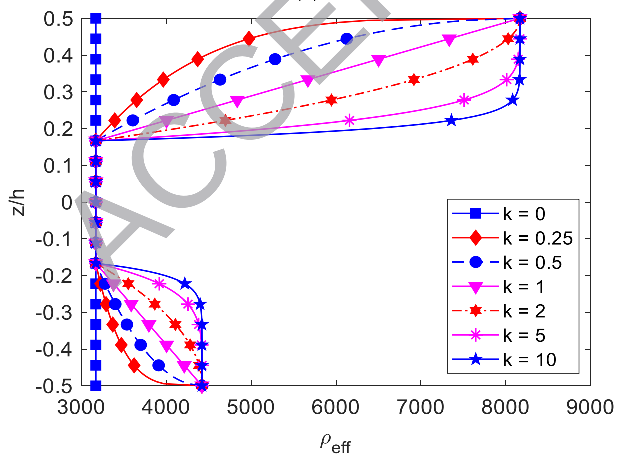

(b)

Fig. 2 The variation of effective Young's modulus and mass density through the thickness of (Ti-6AI-4v/Si_3N_4/SUS304) bi-FGSW nanobeam

density and Poison's ratio of the ceramic component, E_m^1, ρ_m^1, ν_m^1 denote Young's modulus, the mass density and Poison's ratio of the metal component at the bottom surface of the nanobeams, while E_m^2, ρ_m^2, ν_m^2 denote Young's modulus, the mass density and Poison's ratio of the metal component at the top surface of the nanobeams. Table 1 gives the material properties of three individual materials which are used in this study.

The effective Young's modulus (E_{eff}) and mass density (ρ_{eff}) of the material through the thickness of a (Ti-6AI-4v/Si_3N_4/SUS304) bi-FGSW nanobeam with the skin-core-skin thicknesses of (1-1-1) are presented in Fig. 2. It can be seen that when the power-law index k = 0, the bi-FGSW beam becomes the isotropic ceramic one. When the power-law index k > 0, the sandwich beam consists of one core layer of Si_3N_4, one bottom FGM layer of Ti-6AI-4v/Si_3N_4 and one top FGM layer of Si_3N_4/SUS304. The effective material properties of the bi-FGSW nanobeams are asymmetric although the skin-core-skin thicknesses of the beams are symmetric.

2.2 A refined simple shear deformation theory

The basic assumption used in the proposed theory is that the transverse displacement is separated into two parts including bending part w_b and shear part w_s. Thus, the displacement field of the proposed theory can be written as (Nguyen and Nguyen 2015, Nguyen *et al*. 2015)

$$u(x,z) = u(x) - z\frac{\partial w_b}{\partial x} - f(z)\frac{\partial w_s}{\partial x}$$
$$w(x,z) = w_b(x) + w_s(x) \tag{3}$$

where $f(z) = z - r(z)$. Numerous shape functions $r(z)$ have been announced in the past by researchers. In this study, a novel fractional shape function is introduced as follows

$$r(z) = \frac{z}{1 + \frac{16}{7h^2}\left(\frac{z^4}{h^2} + z^2\right)} \tag{4}$$

The current shape fractional shape function satisfies the parabolic distribution of the transverse shear stress/strain through the thickness of the beams and equals to zero on the bottom and top surfaces of the beams. The strains fields of the beam are written as

$$\varepsilon_x = \frac{\partial u}{\partial x} - z\frac{\partial^2 w_b}{\partial x^2} - f\frac{\partial^2 w_s}{\partial x^2},\ \gamma_{xz} = r'\frac{\partial w_s}{\partial x} \tag{5}$$

The constitutive equation of the beam is

$$\sigma_x = E(z)\varepsilon_x, \tau_{xz} = G(z)\gamma_{xz} \tag{6}$$

where $G(z) = E(z)/\left(2(1+\nu(z))\right)$.

The Hamilton's principle is employed to obtained the equations of motion

$$0 = \int_0^T \left(\delta\Pi + \delta V - \delta T\right)dt \tag{7}$$

where $\delta\Pi$ is the variation of the strain energy, δV is the variation of the work done by external forces and δT is the variation of the kinematic energy. The variation of the strain energy is obtained as the following expression

$$\delta\Pi = \int_0^L \int_A \left(\sigma_x \delta\varepsilon_x + \tau_{xz}\delta\gamma_{xz}\right) dAdx \tag{8}$$

After integrating through the thickness of the beam, one gets

$$\delta\Pi = \int_0^L \begin{pmatrix} N^{(l)} \dfrac{\partial \delta u}{\partial x} - M^{(l)} \dfrac{\partial^2 \delta w_b}{\partial x^2} - \\ P^{(l)} \dfrac{\partial^2 \delta w_s}{\partial x^2} + Q^{(l)} \dfrac{\partial \delta w_s}{\partial x} \end{pmatrix} dx \tag{9}$$

where $N^{(l)}, M^{(l)}, P^{(l)}$ and $Q^{(l)}$ are the local stress resultants which are calculated by

$$\left(N, M, P\right)^{(l)} = \int_A \left(1, z, f\right)\sigma_x dA,\ Q = \int_A \sigma_{xz} r' dA \tag{10}$$

Inserting Eq. (6) into Eq. (10), one gets

$$\begin{Bmatrix} N \\ M \\ P \end{Bmatrix}^{(l)} = \begin{bmatrix} A & B & X \\ B & D & F \\ X & F & H \end{bmatrix} \begin{Bmatrix} \dfrac{\partial u}{\partial x} \\ -\dfrac{\partial^2 w_b}{\partial x^2} \\ -\dfrac{\partial^2 w_s}{\partial x^2} \end{Bmatrix},\ Q^{(l)} = S\frac{\partial w_s}{\partial x} \tag{11}$$

where

$$\begin{aligned} &\left(A, B, X, D, F, H\right) = \int_A E(z)\left(1, z, f, z^2, fz, f^2\right) dA, \\ &S = \int_A G(z) r'^2 dA \end{aligned} \tag{12}$$

The variation of the work done by external transverse distributed and axial force is calculated by (Thai *et al*. 2012)

$$\begin{aligned} \delta V = &-\int_0^L q\delta\left(w_b + w_s\right) dx - \\ &\int_0^L N_0 \frac{d\left(w_b + w_s\right)}{dx} \frac{d\delta\left(w_b + w_s\right)}{dx} dx \end{aligned} \tag{13}$$

The variation kinematic energy of the beam is expressed as

$$\delta T = \int_0^L \int_A \begin{bmatrix} \left(\dot{u} - z\dfrac{\partial \dot{w}_b}{\partial x} - f\dfrac{\partial \dot{w}_s}{\partial x}\right) \times \\ \left(\delta\dot{u} - z\dfrac{\partial \delta\dot{w}_b}{\partial x} - f\dfrac{\partial \delta\dot{w}_s}{\partial x}\right) \\ +\left(\dot{w}_b + \dot{w}_s\right)\left(\delta\dot{w}_b + \delta\dot{w}_s\right) \end{bmatrix} \rho(z) dAdx \tag{14}$$

After integrating through the thickness of the beam, one gets

$$\delta T = \int_0^L \begin{bmatrix} I_0\left(\dot{u}\delta\dot{u} + (\dot{w}_b + \dot{w}_s)\delta(\dot{w}_b + \dot{w}_s)\right) + \\ I_1\left(\dot{u}\dfrac{\partial \delta\dot{w}_b}{\partial x} + \dfrac{\partial \dot{w}_b}{\partial x}\delta\dot{u}\right) + \\ I_2\left(\dot{u}\dfrac{\partial \delta\dot{w}_s}{\partial x} + \dfrac{\partial \dot{w}_s}{\partial x}\delta\dot{u}\right) + \\ I_3\left(\dfrac{\partial \dot{w}_b}{\partial x}\dfrac{\partial \delta\dot{w}_b}{\partial x}\right) + \\ I_4\left(\dfrac{\partial \dot{w}_b}{\partial x}\dfrac{\partial \delta\dot{w}_s}{\partial x} + \dfrac{\partial \dot{w}_s}{\partial x}\dfrac{\partial \delta\dot{w}_b}{\partial x}\right) + \\ +I_5\left(\dfrac{\partial \dot{w}_s}{\partial x}\dfrac{\partial \delta\dot{w}_s}{\partial x}\right) \end{bmatrix} dx \tag{15}$$

where

$$\left(I_0, I_1, I_2, I_3, I_4, I_5\right) = \int_A \rho(z)\left(1, -z, -f, z^2, fz, f^2\right) dA \tag{16}$$

Substituting Eqs. (9), (13) and Eq. (15) into Eq. (7) and integrating by parts, the equilibrium equations of the beams are obtained as the following

$$\begin{aligned} &\delta u: -\frac{\partial N^{(l)}}{\partial x} = -I_0\ddot{u} - I_1\frac{\partial \ddot{w}_b}{\partial x} - I_2\frac{\partial \ddot{w}_s}{\partial x}, \\ &\delta w_b: -\frac{\partial^2 M^{(l)}}{\partial x^2} = q - N_0\frac{d^2(w_b + w_s)}{dx^2} - \\ &\qquad I_0(\ddot{w}_b + \ddot{w}_s) + I_1\frac{\partial \ddot{u}}{\partial x} + I_3\frac{\partial^2 \ddot{w}_b}{\partial x^2} + I_4\frac{\partial^2 \ddot{w}_s}{\partial x^2}, \\ &\delta w_s: -\frac{\partial^2 P^{(l)}}{\partial x^2} - \frac{\partial Q^{(l)}}{\partial x} = q - N_0\frac{d^2(w_b + w_s)}{dx^2} - \\ &\qquad I_0\left(\ddot{w}_b + \ddot{w}_s\right) + I_2\frac{\partial \ddot{u}}{\partial x} + I_4\frac{\partial^2 \ddot{w}_b}{\partial x^2} + I_5\frac{\partial^2 \ddot{w}_s}{\partial x^2}. \end{aligned} \tag{17}$$

2.3 Nonlocal theory

To take into account for the small-scale effects on the behavior of the nanobeams, the Eringen's nonlocal theory (Eringen, 1983) is adopted herein. In the Eringen's nonlocal theory, the stress at a point depends on the strains at all neighbor points of the body, hence the nonlocal stress tensor σ_{ij} at a point x is obtained via the local stress tensor t_{ij} as the following formula (Aria and Friswell 2019)

$$\sigma_{ij} - \mu\nabla^2\sigma_{ij} = t_{ij} \tag{18}$$

where $\mu = (e_0 a)^2$ is the nonlocal parameter which incorporates the small-scale effect, e_0 is a constant appropriate to each material which can be obtained either from experimental measurements or molecular dynamics, a is the internal characteristic length. For a beam type structure, by considering the nonlocal behavior in the thickness direction, the softening effect will depend on the span to depth ratio, in addition to the nonlocal parameter. In this study, the nonlocal effect in the thickness direction is ignored, and so the softening behavior is only dependent on the nonlocal parameter. Besides, by letting $\mu = 0$, the constitutive relation for the local theory is derived. The nonlocal constitutive relation of the nanobeams can be written as (Hamed *et al*. 2016)

$$\left(1-\mu\nabla^2\right)\begin{Bmatrix}\sigma_x\\ \tau_{xz}\end{Bmatrix}=\begin{bmatrix}E(z) & 0\\ 0 & G(z)\end{bmatrix}\begin{Bmatrix}\varepsilon_x\\ \gamma_{xz}\end{Bmatrix} \tag{19}$$

As a consequence, the stress resultants are calculated as the following formula

$$\left(1-\mu\nabla^2\right)\begin{Bmatrix}N\\ M\\ P\end{Bmatrix}=\begin{bmatrix}A & B & X\\ B & D & F\\ X & F & H\end{bmatrix}\begin{Bmatrix}\dfrac{\partial u}{\partial x}\\ -\dfrac{\partial^2 w_b}{\partial x^2}\\ -\dfrac{\partial^2 w_s}{\partial x^2}\end{Bmatrix}, \qquad Q-\mu\nabla^2 Q = S\frac{\partial w_s}{\partial x} \tag{20}$$

2.4 Equations of motion

By substituting Eq. (20) into Eq. (17), the following equations of motion of the nanobeams are achieved as the following formulae

$$\begin{aligned}
&\delta u: A\frac{\partial^2 u}{\partial x^2}-B\frac{\partial^3 w_b}{\partial x^3}-X\frac{\partial^3 w_s}{\partial x^3}=\\
&=\left(1-\mu\nabla^2\right)\left(I_0\ddot{u}+I_1\frac{\partial \ddot{w}_b}{\partial x}+I_2\frac{\partial \ddot{w}_s}{\partial x}\right),\\
&\delta w_b: B\frac{\partial^3 u}{\partial x^3}-D\frac{\partial^4 w_b}{\partial x^4}-F\frac{\partial^4 w_s}{\partial x^4}=\\
&=\left(1-\mu\nabla^2\right)\left(\begin{array}{l}-q+N_0\dfrac{d^2(w_b+w_s)}{dx^2}+\\ I_0(\ddot{w}_b+\ddot{w}_s)-I_1\dfrac{\partial \ddot{u}}{\partial x}-\\ I_3\dfrac{\partial^2 \ddot{w}_b}{\partial x^2}-I_4\dfrac{\partial^2 \ddot{w}_s}{\partial x^2}\end{array}\right),\\
&\delta w_s: X\frac{\partial^3 u}{\partial x^3}-F\frac{\partial^4 w_b}{\partial x^4}-H\frac{\partial^4 w_s}{\partial x^4}+S\frac{\partial^2 w_s}{\partial x^2}=\\
&=\left(1-\mu\nabla^2\right)\left(\begin{array}{l}-q+N_0\dfrac{d^2(w_b+w_s)}{dx^2}+\\ I_0\left(\ddot{w}_b+\ddot{w}_s\right)-I_2\dfrac{\partial \ddot{u}}{\partial x}-\\ I_4\dfrac{\partial^2 \ddot{w}_b}{\partial x^2}-I_5\dfrac{\partial^2 \ddot{w}_s}{\partial x^2}\end{array}\right).
\end{aligned} \tag{21}$$

2.5 Navier's solution

In this study, a simply-simply supported bi-FGSW nanobeam subjected to a distributed transverse load is considered. The simply supported boundary conditions of the beams are

$$w_b = w_s = N = M = P = 0 \quad \text{at} \quad x = 0, L \tag{22}$$

The Navier's solution technique is employed to solve the equations of motion. The unknown displacement functions of the beams are assumed as the following formulae

$$\begin{Bmatrix}u(x,t)\\ w_b(x,t)\\ w_s(x,t)\end{Bmatrix}=\sum_{m=1}^{\infty}\begin{Bmatrix}U_m e^{i\omega t}\cos\alpha_m x\\ Wb_m e^{i\omega t}\sin\alpha_m x\\ Ws_m e^{i\omega t}\sin\alpha_m x\end{Bmatrix} \tag{23}$$

where $\alpha_m = m\pi / L$, $i^2 = -1$, ω is the natural frequency of the nanobeams, U_m, Wb_m, Ws_m are the unknown coefficients. The distributed load acting on the beam is expanded as follows

$$q(x)=\sum_{m=1}^{\infty}\Omega_m \sin\alpha_m x \tag{24}$$

where Ω_m depends on the load types. In the case of uniform load, Ω_m are calculated by

$$\Omega_m=\begin{cases}\dfrac{4q_0}{m\pi} & m \text{ even}\\ 0 & m \text{ odd}\end{cases} \tag{25}$$

Substituting Eq. (23) and Eq. (24) into Eq. (21), one gets

$$\left(\begin{array}{l}\begin{bmatrix}k_{11} & k_{12} & k_{13}\\ & k_{22} & k_{23}\\ sys & & k_{33}\end{bmatrix}-\\ \vartheta N_0\alpha_m^2\begin{bmatrix}0 & 0 & 0\\ 0 & 1 & 1\\ 0 & 1 & 1\end{bmatrix}-\\ \vartheta\omega^2\begin{bmatrix}m_{11} & m_{12} & m_{13}\\ & m_{22} & m_{23}\\ sys & & m_{33}\end{bmatrix}\end{array}\right)\begin{Bmatrix}U_m\\ Wb_m\\ Ws_m\end{Bmatrix}=\vartheta\begin{Bmatrix}0\\ \Omega_m\\ \Omega_m\end{Bmatrix} \tag{26}$$

where $\vartheta=\left(\alpha_m^2\mu+1\right)$ and

$$\begin{aligned}
&k_{11}=\alpha_m^2 A;\, k_{12}=-\alpha_m^3 B;\, k_{13}=-X\alpha_m^3;\\
&k_{22}=\alpha_m^4 D;\, k_{23}=\alpha_m^4 F;\, k_{33}=\alpha_m^2\left(H\alpha_m^2+S\right);\\
&m_{11}=I_0;\, m_{12}=I_1\alpha_m;\\
&m_{13}=I_2\alpha_m;\, m_{22}=I_3\alpha_m^2+I_0;\\
&m_{23}=I_4\alpha_m^2+I_0;\, m_{33}=I_5\alpha_m^2+I_0.
\end{aligned} \tag{27}$$

The numerical results of the bending behavior, frequencies and critical buckling load of the bi-FGSW nanobeams are obtained by solving Eq. (26) using a common manner. The static deflection is obtained from Eq. (26) by setting N_0 and ω equal to zero. The natural frequency is obtained from Eq. (26) by setting q and N_0 equal to zero. By setting q and ω in Eq. (26) equal to zero, the critical buckling load is obtained.

3. Numerical results and discussions

3.1 Verification study

3.1.1 Comparison the bending, free vibration and buckling of FGSW beams

The FGSW beams are made of one homogeneous Al_2O_3 core and two FGM faces of Al_2O_3/Al. The material properties of Aluminum (Al) as metal are $E_m = 70\,\text{GPa}$, $\nu_m = 0.3$, $\rho_m = 2702\,\text{kg/m}^3$ and those of Alumina (Al_2O_3) as ceramic are $E_c = 380\,\text{GPa}$, $\nu_c = 0.3$, $\rho_c = 3960\,\text{kg/m}^3$. The dimensionless center deflections, normal stress and transverse shear stress of simply-simply supported FGSW beams subjected to uniform load q_0 are compared in Tables 2-4. In which the numerical results of the proposed theory are compared to those of Nguyen and Nguyen (2015). Furthermore, the comparison of the dimensionless fundamental frequencies and critical buckling loads between the present numerical results and those of Nguyen and Nguyen (2015) are presented in Tables 5 and 6. According to these comparisons, it can be concluded that the present numerical results are identical to those of Nguyen and Nguyen (2015). In these tables, the dimensionless parameters are calculated via following formulae

$$\begin{aligned}
&\bar{w} = \frac{h^3}{12}\frac{384E_m}{5q_0L^4}w,\ \bar{\omega} = \omega\frac{L^2}{h}\sqrt{\frac{\rho_m}{E_m}},\ \bar{N}_{cr} = N_{cr}\frac{12L^2}{E_m h^3},\\
&\bar{\sigma}_x(z) = \sigma_x\left(\frac{L}{2},z\right)\frac{h}{q_0L},\ \bar{\tau}_{xz}(z) = \tau_{xz}\left(0,z\right)\frac{h}{q_0L}.
\end{aligned} \tag{28}$$

3.1.2 Comparison the bending, free vibration and buckling of isotropic nanobeams

To verify the accuracy of the proposed theory on predicting the bending, free vibration and buckling behavior of nanostructures, the comparisons of the deflections, fundamental frequencies and critical buckling loads of a simply supports isotropic nanobeams are considered herein. The length of the beam is $L = 10\,\text{nm}$ and it is subjected to a uniform load. The present numerical results are compared with those of Thai and Vo (2012) for several cases of the slender ratios and the nonlocal parameters. It can be seen from Table 7 that the errors between the present results and those of Thai and Vo (2012) are very small. It is noticed that the dimensionless center deflections, natural frequencies and critical buckling loads are computed as the following formulae

$$\begin{aligned}
&\bar{w} = \frac{100EI}{q_0L^4}w,\ \bar{\omega} = \omega L^2\sqrt{\frac{m_0}{EI}},\ \bar{N}_{cr} = \frac{L^2}{EI}N_{cr},\\
&I = \frac{bh^3}{12},\ m_0 = \rho bh
\end{aligned} \tag{29}$$

3.2. Parameter study

In this section, the bending behavior, free vibration and buckling behavior of the (Ti-6AI-4v/Si_3N_4/SUS304) bi-FGSW nanobeams are investigated. The length of nanobeam is $L = 10\,\text{nm}$, the depth of the nanobeam is $b = 1\,\text{nm}$, the beam is simply supported at two end sides. For the bending problems, the nanobeam is subjected to a uniform load, for the free vibration problems, the nanobeam is free of force action, and for the buckling problems, the nanobeam is subjected to axial load only. The following dimensionless quantities are used for convenience

$$\begin{aligned}
&w^*(z) = \frac{10^2E_0h_0^3}{12L^4q}w\left(\frac{L}{2}\right),\ \sigma_x^*(z) = \frac{h_0}{Lq}\sigma_x\left(\frac{L}{2},z\right),\\
&\tau_{xz}^*(z) = \frac{h_0}{Lq}\tau_{xz}\left(0,z\right),\ \omega^* = \omega L^2\sqrt{\frac{12\rho_0}{h_0^2E_0}},\\
&N_{cr}^* = N_{cr}\frac{12L^2}{E_0h_0^3},\ E_0 = 200\,\text{GPa},\\
&\rho_0 = 3000\,\text{kg/m}^3,\ h_0 = L/10.
\end{aligned} \tag{30}$$

3.2.1 The bending analysis of bi-FGSW nanobeams

Firstly, the bending behavior of the (Ti-6AI-4v/Si_3N_4/SUS304) bi-FGSW nanobeam is investigated in this subsection. The nondimensional center deflection, the axial normal stress and the transverse shear stress of the bi- FGSW nanobeam subjected to a uniform distribution load q are presented in Tables 8-10. It can be seen that the deflections of the bi-FGSW nanobeams increase as the growth of the length-to-high ratio L/h, the power-law index k as well as the nonlocal parameter μ. When the power-law index $k = 0$, the deflections and stresses of six schemes of the sandwich nanobeams are identical because they become the full-ceramic ones.

Continuously, the effects of some parameters such as slender ratio L/h, the power-law index k, and the nonlocal parameter μ on the bending behavior of the bi-FGSW nanobeams are investigated herein for details. A bi-FGSW nanobeam with two simply supported end sides is considered. The deflection of the (1-2-1) bi-FGSW nanobeams with different values of the power-law index k and the nonlocal parameter μ are presented in Fig. 3(a). The dependence of the center deflections of the (1-1-1) bi-FGSW nanobeams on the variation of the slender ratio L/h are given in Fig. 3(b). It is obvious that the center deflections of the beams are increased as the growth of the slender ratio. The rate of increase of the beams with

Table 2 The comparison of the center deflection $\bar{w}$ of the FGSW beams

L/h	*k*	Method	1-0-1	2-1-2	2-1-1	1-1-1	2-2-1	1-2-1
5	0	Nguyen and Nguyen (2015)	0.2026	0.2026	0.2026	0.2026	0.2026	0.2026
		Present	0.2024	0.2024	0.2024	0.2024	0.2024	0.2024
	1	Nguyen and Nguyen (2015)	0.5014	0.4437	0.4189	0.4012	0.3738	0.3464
		Present	0.5007	0.4431	0.4185	0.4009	0.3736	0.3463
	5	Nguyen and Nguyen (2015)	0.9714	0.8450	0.7568	0.7185	0.6267	0.5449
		Present	0.9680	0.8429	0.7556	0.7174	0.6260	0.5447
	10	Nguyen and Nguyen (2015)	1.0425	0.9359	0.8329	0.8042	0.6943	0.6019
		Present	1.0380	0.9330	0.8314	0.8026	0.6934	0.6016
20	0	Nguyen and Nguyen (2015)	0.1854	0.1854	0.1854	0.1854	0.1854	0.1854
		Present	0.1853	0.1853	0.1853	0.1853	0.1853	0.1853
	1	Nguyen and Nguyen (2015)	0.4763	0.4214	0.3967	0.3802	0.3530	0.3264
		Present	0.4762	0.4213	0.3966	0.3801	0.3530	0.3264
	5	Nguyen and Nguyen (2015)	0.9295	0.8164	0.7282	0.6936	0.6024	0.5225
		Present	0.9293	0.8163	0.7282	0.6935	0.6023	0.5225
	10	Nguyen and Nguyen (2015)	0.9884	0.9048	0.8018	0.7782	0.6690	0.5790
		Present	0.9881	0.9046	0.8017	0.7781	0.6689	0.5790

Table 3 The comparison of the normal stress $\bar{\sigma}_x(z=h/2)$ of the FGSW beams

L/h	*k*	Method	1-0-1	2-1-2	2-1-1	1-1-1	2-2-1	1-2-1
5	0	Nguyen and Nguyen (2015)	3.8022	3.8022	3.8022	3.8022	3.8022	3.8022
		Present	3.7517	3.7517	3.7517	3.7517	3.7517	3.7517
	1	Nguyen and Nguyen (2015)	1.7967	1.5898	1.3885	1.4349	1.2475	1.2330
		Present	1.7846	1.5793	1.3780	1.4251	1.2377	1.2236
	5	Nguyen and Nguyen (2015)	3.5001	3.0730	2.4070	2.6124	2.0195	1.9706
		Present	3.4785	3.0591	2.3938	2.6010	2.0085	1.9610
	10	Nguyen and Nguyen (2015)	3.7235	3.4044	2.6296	2.9294	2.2200	2.1827
		Present	3.6946	3.3886	2.6151	2.9172	2.2085	2.1729
20	0	Nguyen and Nguyen (2015)	15.0130	15.0130	15.0130	15.0130	15.0130	15.0130
		Present	15.0232	15.0232	15.0232	15.0232	15.0232	15.0232
	1	Nguyen and Nguyen (2015)	7.1229	6.3018	5.4960	5.6850	4.9364	4.8801
		Present	7.1256	6.3042	5.4985	5.6873	4.9387	4.8823
	5	Nguyen and Nguyen (2015)	13.9065	12.2220	9.5507	10.3835	8.0109	7.8194
		Present	13.9108	12.2248	9.5539	10.3862	8.0136	7.8220
	10	Nguyen and Nguyen (2015)	14.7788	13.5456	10.4356	11.6513	8.8104	8.6665
		Present	14.7839	13.5483	10.4390	11.6539	8.8132	8.6692

Table 4 The comparison of the transverse shear stress $\bar{\tau}_{xz}(z=0)$ of the FGSW beams

L/h	*k*	Method	1-0-1	2-1-2	2-1-1	1-1-1	2-2-1	1-2-1
5	0	Nguyen and Nguyen (2015)	0.7350	0.7350	0.7350	0.7350	0.7350	0.7350
		Present	0.7924	0.7924	0.7924	0.7924	0.7924	0.7924
	1	Nguyen and Nguyen (2015)	1.0349	0.9139	0.9106	0.8602	0.8496	0.8141
		Present	1.0845	0.9623	0.9672	0.9131	0.9067	0.8744
	5	Nguyen and Nguyen (2015)	1.7725	1.1854	1.1755	1.0133	0.9873	0.8940
		Present	1.7791	1.1918	1.2187	1.0403	1.0316	0.9467
	10	Nguyen and Nguyen (2015)	2.3128	1.3065	1.2888	1.0670	1.0347	0.9165

Table 4 Continued

L/h	k	Method	1-0-1	2-1-2	2-1-1	1-1-1	2-2-1	1-2-1
5	10	Present	2.3312	1.2942	1.3306	1.0808	1.0735	0.9635
20	0	Nguyen and Nguyen (2015)	0.7470	0.7470	0.7470	0.7470	0.7470	0.7470
		Present	0.8102	0.8102	0.8102	0.8102	0.8102	0.8102
	1	Nguyen and Nguyen (2015)	1.0466	0.9241	0.9209	0.8699	0.8594	0.8235
		Present	1.1023	0.9780	0.9833	0.9282	0.9220	0.8893
	5	Nguyen and Nguyen (2015)	1.7927	1.1976	1.1877	1.0237	0.9972	0.9030
		Present	1.8075	1.2095	1.2370	1.0560	1.0469	0.9609
	10	Nguyen and Nguyen (2015)	2.3411	1.3196	1.3023	1.0779	1.0450	0.9258
		Present	2.3705	1.3130	1.3507	1.0970	1.0892	0.9780

Table 5 The comparison of the natural frequency $\bar{\varpi}$ of the FGSW beams

L/h	k	Method	1-0-1	2-1-2	2-1-1	1-1-1	2-2-1	1-2-1
5	0	Nguyen and Nguyen (2015)	5.1528	5.1528	5.1528	5.1528	5.1528	5.1528
		Present	5.1556	5.1556	5.1556	5.1556	5.1556	5.1556
	1	Nguyen and Nguyen (2015)	3.5735	3.7298	3.8206	3.8756	3.9911	4.1105
		Present	3.5762	3.7320	3.8221	3.8770	3.9922	4.1108
	5	Nguyen and Nguyen (2015)	2.7448	2.8440	2.9789	3.0181	3.1965	3.3771
		Present	2.7495	2.8473	2.9811	3.0204	3.1982	3.3775
	10	Nguyen and Nguyen (2015)	2.6934	2.7356	2.8715	2.8809	3.0629	3.2357
		Present	2.6990	2.7396	2.8740	2.8836	3.0649	3.2365
20	0	Nguyen and Nguyen (2015)	5.4603	5.4603	5.4603	5.4603	5.4603	5.4603
		Present	5.4605	5.4605	5.4605	5.4605	5.4605	5.4605
	1	Nguyen and Nguyen (2015)	3.7147	3.8768	3.9775	4.0328	4.1603	4.2889
		Present	3.7149	3.8769	3.9776	4.0329	4.1603	4.2889
	5	Nguyen and Nguyen (2015)	2.8440	2.9311	3.0776	3.1111	3.3030	3.4921
		Present	2.8443	2.9313	3.0777	3.1112	3.3031	3.4922
	10	Nguyen and Nguyen (2015)	2.8042	2.8188	2.9665	2.9662	3.1616	3.3406
		Present	2.8046	2.8191	2.9666	2.9664	3.1617	3.3407

Table 6 The comparison of the critical buckling load $\bar{N}_{cr}$ of the FGSW beams

L/h	k	Method	1-0-1	2-1-2	2-1-1	1-1-1	2-2-1	1-2-1
5	0	Nguyen and Nguyen (2015)	48.5960	48.5960	48.5960	48.5960	48.5960	48.5960
		Present	48.6534	48.6534	48.6534	48.6534	48.6534	48.6534
	1	Nguyen and Nguyen (2015)	19.6531	22.2113	23.5246	24.5598	26.3609	28.4444
		Present	19.6841	22.2391	23.5451	24.5798	26.3774	28.4497
	5	Nguyen and Nguyen (2015)	10.1473	11.6685	13.0272	13.7218	15.7307	18.0914
		Present	10.1841	11.6979	13.0477	13.7435	15.7483	18.0975
	10	Nguyen and Nguyen (2015)	9.4526	10.5356	11.8372	12.2611	14.1995	16.3787
		Present	9.4943	10.5689	11.8588	12.2858	14.2192	16.3879
20	0	Nguyen and Nguyen (2015)	53.2364	53.2364	53.2364	53.2364	53.2364	53.2364
		Present	53.2405	53.2405	53.2405	53.2405	53.2405	53.2405
	1	Nguyen and Nguyen (2015)	20.7213	23.4212	24.8793	25.9588	27.9537	30.2307
		Present	20.7234	23.4231	24.8807	25.9602	27.9549	30.2310
	5	Nguyen and Nguyen (2015)	10.6175	12.0885	13.5519	14.2285	16.3829	18.8874
		Present	10.6197	12.0904	13.5532	14.2299	16.3841	18.8878

Table 6 Continued

L/h	k	Method	1-0-1	2-1-2	2-1-1	1-1-1	2-2-1	1-2-1
20	10	Nguyen and Nguyen (2015)	9.9849	10.9074	12.3080	12.6819	14.7520	17.0445
		Present	9.9877	10.9098	12.3094	12.6836	14.7532	17.0449

Table 7 The comparison of the center deflection $\bar{w}$, frequency $\bar{\varpi}$ and critical buckling load $\bar{N}_{cr}$ of the isotropic nanobeams

L/h	$\mu(\mathrm{nm}^2)$	$\bar{w}$		$\bar{\varpi}$		$\bar{N}_{cr}$	
		Thai and Vo (2012)	Present	Thai and Vo (2012)	Present	Thai and Vo (2012)	Present
5	0	1.4317	1.4303	9.2752	9.2797	8.9533	8.9625
	1	1.5671	1.5656	8.8488	8.8531	8.1490	8.1574
	2	1.7025	1.7009	8.4763	8.4804	7.4773	7.4850
	4	1.9733	1.9714	7.8536	7.8574	6.4191	6.4257
10	0	1.3345	1.3342	9.7077	9.7090	9.6231	9.6257
	1	1.4621	1.4617	9.2614	9.2626	8.7587	8.7610
	2	1.5897	1.5893	8.8715	8.8727	8.0367	8.0389
	4	1.8449	1.8445	8.2198	8.2209	6.8994	6.9012
100	0	1.3024	1.3024	9.8679	9.8680	9.8671	9.8671
	1	1.4274	1.4274	9.4143	9.4143	8.9807	8.9808
	2	1.5525	1.5525	9.0180	9.0180	8.2405	8.2405
	4	1.8025	1.8025	8.3555	8.3555	7.0743	7.0743

Table 8 The dimensionless center deflection w^* of the bi-FGSW nanobeams

L/h	k	$\mu(\mathrm{nm}^2)$	1-0-1	2-1-2	2-1-1	1-1-1	2-2-1	1-2-1
5	0	0	0.1107	0.1107	0.1107	0.1107	0.1107	0.1107
		1	0.1212	0.1212	0.1212	0.1212	0.1212	0.1212
		2	0.1316	0.1316	0.1316	0.1316	0.1316	0.1316
		3	0.1421	0.1421	0.1421	0.1421	0.1421	0.1421
		4	0.1526	0.1526	0.1526	0.1526	0.1526	0.1526
	1	0	0.1974	0.1833	0.1886	0.1725	0.1746	0.1578
		1	0.2162	0.2007	0.2065	0.1889	0.1912	0.1728
		2	0.2350	0.2181	0.2244	0.2053	0.2077	0.1878
		3	0.2537	0.2355	0.2423	0.2217	0.2243	0.2027
		4	0.2725	0.2529	0.2602	0.2381	0.2409	0.2177
	10	0	0.3044	0.2754	0.2958	0.2513	0.2640	0.2154
		1	0.3333	0.3017	0.3239	0.2753	0.2891	0.2359
		2	0.3623	0.3279	0.3521	0.2992	0.3142	0.2564
		3	0.3912	0.3541	0.3802	0.3231	0.3394	0.2769
		4	0.4201	0.3803	0.4084	0.3471	0.3645	0.2974
10	0	0	0.8261	0.8261	0.8261	0.8261	0.8261	0.8261
		1	0.9051	0.9051	0.9051	0.9051	0.9051	0.9051
		2	0.9841	0.9841	0.9841	0.9841	0.9841	0.9841
		3	1.0631	1.0631	1.0631	1.0631	1.0631	1.0631
		4	1.1421	1.1421	1.1421	1.1421	1.1421	1.1421
	1	0	1.5046	1.3967	1.4369	1.3129	1.3286	1.1969
		1	1.6486	1.5304	1.5745	1.4386	1.4558	1.3114
		2	1.7927	1.6641	1.7121	1.5643	1.5830	1.4260
		3	1.9367	1.7978	1.8496	1.6900	1.7101	1.5405
		4	2.0807	1.9315	1.9872	1.8156	1.8373	1.6550

Table 8 Continued

L/h	k	$\mu(\mathrm{nm}^2)$	1-0-1	2-1-2	2-1-1	1-1-1	2-2-1	1-2-1
	10	0	2.3256	2.1221	2.2762	1.9369	2.0359	1.6535
		1	2.5482	2.3254	2.4942	2.1225	2.2310	1.8119
10		2	2.7709	2.5287	2.7123	2.3080	2.4260	1.9703
		3	2.9936	2.7320	2.9303	2.4936	2.6211	2.1287
		4	3.2162	2.9353	3.1484	2.6791	2.8161	2.2870

Table 9 The dimensionless normal stress $\sigma_x^*(L/2, h/2)$ of the bi-FGSW nanobeams

L/h	k	$\mu(\mathrm{nm}^2)$	1-0-1	2-1-2	2-1-1	1-1-1	2-2-1	1-2-1
	0	0	1.9230	1.9230	1.9230	1.9230	1.9230	1.9230
		1	2.0655	2.0655	2.0655	2.0655	2.0655	2.0655
		2	2.2079	2.2079	2.2079	2.2079	2.2079	2.2079
		3	2.3503	2.3503	2.3503	2.3503	2.3503	2.3503
		4	2.4928	2.4928	2.4928	2.4928	2.4928	2.4928
	1	0	2.0208	1.9149	1.8807	1.8257	1.7771	1.6944
		1	2.1705	2.0568	2.0197	1.9609	1.9083	1.8194
5		2	2.3202	2.1987	2.1587	2.0960	2.0396	1.9445
		3	2.4700	2.3407	2.2976	2.2312	2.1708	2.0696
		4	2.6197	2.4826	2.4366	2.3663	2.3020	2.1946
	10	0	2.6994	2.6255	2.5989	2.4879	2.4363	2.2170
		1	2.8992	2.8218	2.7922	2.6744	2.6181	2.3825
		2	3.0990	3.0181	2.9855	2.8609	2.7999	2.5480
		3	3.2989	3.2144	3.1788	3.0474	2.9817	2.7135
		4	3.4987	3.4107	3.3721	3.2339	3.1636	2.8790
	0	0	7.5480	7.5480	7.5480	7.5480	7.5480	7.5480
		1	8.1187	8.1187	8.1187	8.1187	8.1187	8.1187
		2	8.6894	8.6894	8.6894	8.6894	8.6894	8.6894
		3	9.2601	9.2601	9.2601	9.2601	9.2601	9.2601
		4	9.8308	9.8308	9.8308	9.8308	9.8308	9.8308
	1	0	7.9606	7.5454	7.4041	7.1918	6.9960	6.6690
		1	8.5610	8.1145	7.9614	7.7338	7.5223	7.1706
10		2	9.1614	8.6836	8.5188	8.2758	8.0485	7.6722
		3	9.7618	9.2527	9.0761	8.8178	8.5747	8.1737
		4	10.3622	9.8218	9.6334	9.3598	9.1009	8.6753
	10	0	10.6230	10.3719	10.2471	9.8321	9.6191	8.7518
		1	11.4242	11.1590	11.0221	10.5798	10.3482	9.4154
		2	12.2253	11.9461	11.7971	11.3275	11.0773	10.0789
		3	13.0265	12.7332	12.5722	12.0753	11.8064	10.7425
		4	13.8277	13.5203	13.3472	12.8230	12.5355	11.4061

Table 10 The dimensionless transverse shear stress $\tau_{xz}^*(0,0)$ of the bi-FGSW nanobeams

L/h	k	$\mu(\mathrm{nm}^2)$	1-0-1	2-1-2	2-1-1	1-1-1	2-2-1	1-2-1
	0	0	0.3962	0.3962	0.3962	0.3962	0.3962	0.3962
5		1	0.9167	0.9167	0.9167	0.9167	0.9167	0.9167
		2	1.4372	1.4372	1.4372	1.4372	1.4372	1.4372
		3	1.9577	1.9577	1.9577	1.9577	1.9577	1.9577

Table 10 Continued

L/h	k	$\mu(\text{nm}^2)$	1-0-1	2-1-2	2-1-1	1-1-1	2-2-1	1-2-1
5	0	4	2.4782	2.4782	2.4782	2.4782	2.4782	2.4782
	1	0	0.4867	0.4494	0.4644	0.4338	0.4390	0.4217
		1	1.2198	1.1325	1.1615	1.0908	1.1011	1.0550
		2	1.9529	1.8155	1.8587	1.7477	1.7633	1.6882
		3	2.6860	2.4985	2.5559	2.4046	2.4254	2.3215
		4	3.4192	3.1815	3.2530	3.0616	3.0876	2.9547
	10	0	0.7390	0.5407	0.6022	0.4807	0.4984	0.4443
		1	1.8159	1.3948	1.5141	1.2347	1.2778	1.1316
		2	2.8928	2.2488	2.4260	1.9886	2.0572	1.8190
		3	3.9697	3.1029	3.3379	2.7426	2.8367	2.5063
		4	5.0466	3.9570	4.2499	3.4966	3.6161	3.1936
10	0	0	0.8043	0.8043	0.8043	0.8043	0.8043	0.8043
		1	2.7352	2.7352	2.7352	2.7352	2.7352	2.7352
		2	4.6661	4.6661	4.6661	4.6661	4.6661	4.6661
		3	6.5970	6.5970	6.5970	6.5970	6.5970	6.5970
		4	8.5279	8.5279	8.5279	8.5279	8.5279	8.5279
	1	0	0.9859	0.9103	0.9407	0.8787	0.8892	0.8543
		1	3.6697	3.4083	3.4937	3.2823	3.3128	3.1732
		2	6.3534	5.9063	6.0468	5.6858	5.7364	5.4922
		3	9.0372	8.4043	8.5998	8.0894	8.1601	7.8111
		4	11.7209	10.9024	11.1529	10.4929	10.5837	10.1301
	10	0	1.4976	1.0945	1.2197	0.9731	1.0090	0.8996
		1	5.4535	4.2049	4.5561	3.7211	3.8507	3.4085
		2	9.4094	7.3152	7.8926	6.4691	6.6924	5.9175
		3	13.3653	10.4256	11.2290	9.2172	9.5341	8.4264
		4	17.3212	13.5360	14.5654	11.9652	12.3758	10.9354

$k=0$, and the rate of increase is increased as k increases. In Fig. 3(c), when the power-law index k increases, the center deflections of the nanobeams increases. The reason is that when the power-law index increases, two FGM face sheets of the bi-FGSWnanobeams become metal-rich face sheets, it leads to the decrease of the stiffness of the beams. Besides, the effects of the nonlocal parameter μ on the center deflections of the bi-FGSW nanobeams are demonstrated in Fig. 3(d). It is obvious that the inclusion of the nonlocal parameter leads to an increase in the center deflection of the bi-FGSW nanobeams.

The distribution of normal stress and transverse shear stress through the thickness of the bi-FGSW nanobeams are presented in Figs. 4 and 5. The distribution of the normal stress and transverse shear stress of the bi-FGSW nanobeams with six schemes of sandwich beams are illustrated in Figs. 4(a) and 5(a). The scheme of the sandwich beams affects strongly on the distribution of the stresses through the thickness of the sandwich nanobeams. Furthermore, the distribution of the stresses through the thickness of the bi-FGSW nanobeams are still asymmetric although the schemes of the beams are symmetric. These are due to the fact that the bi-FGSW nanobeams consist of two different FGM face sheets with different ingredients. The influence of the slender ratio on the distribution of the stresses is presented in Figs. 4(b) and 5(b). The effects of the power-law index on the distribution of the tresses are presented in Figs. 4(c) and 5(c). Figs. 4(d) and 5(d) present the effect of the nonlocal parameter on the distribution of the normal and transverse shear stress. It can be seen that the slender ratio, the power-law index and the nonlocal parameter have strong effects on the distribution of the normal and transverse shear stresses in the thickness direction of the bi-FGSW nanobeams. Especially, the distribution of the normal stress at two surfaces of the bi-FGSW nanobeams are always asymmetric, hence the use of the bi-FGSW nanobeams can avoid the phenomenon of stresses concentration at the surfaces of the beams.

3.2.2 Free vibration analysis of bi-FGSW nanobeams

In this subsection, the free vibration analysis of the simply supported bi-FGSW nanobeams is considered. The dimensionless fundamental frequencies of the bi-FGSW nanobeams are given in Table 11. The dimensionless first six frequencies of the (1-0-1) and (2-2-1) bi-FGSW

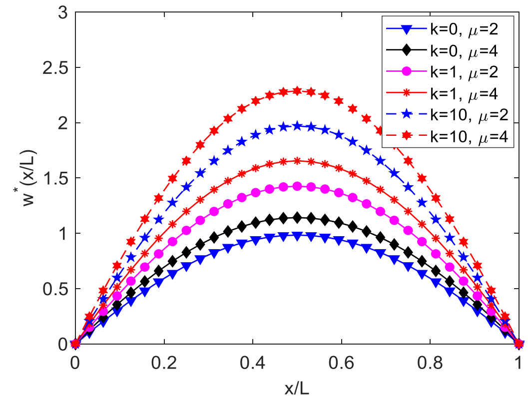

(a) $L/h = 10$, (1-2-1) scheme

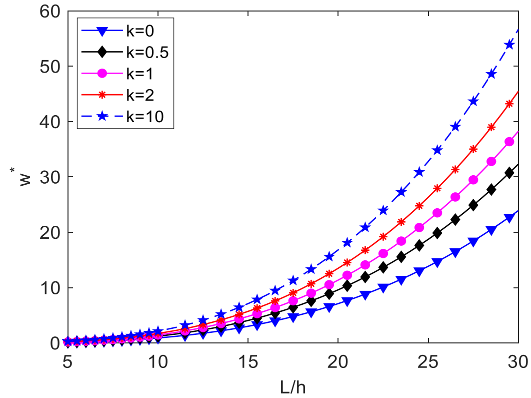

(b) $\mu = 1$, (1-1-1) scheme

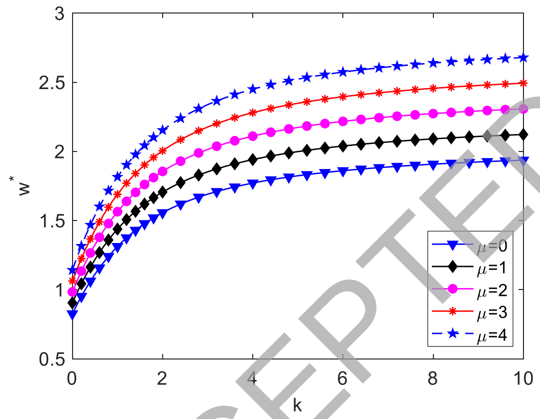

(c) $L/h = 10$, (1-1-1) scheme

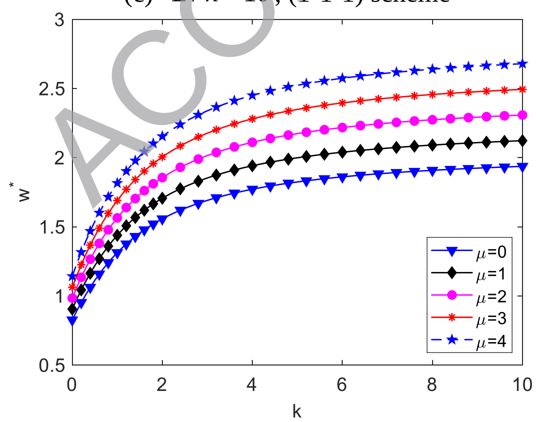

(d) $L/h = 10$, (1-1-1) scheme

Fig. 3 The variation of the dimensionless deflection of the bi-FGSW nanobeams

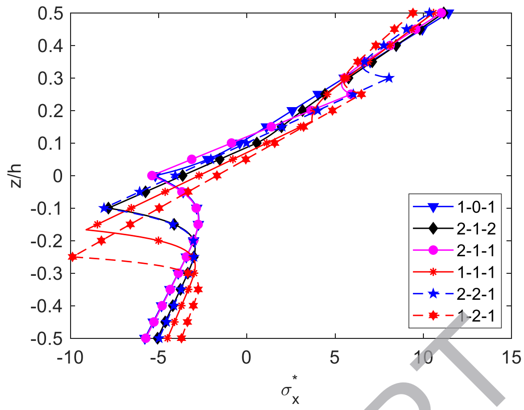

(a) $L/h = 10, k = 10, \mu = 1$

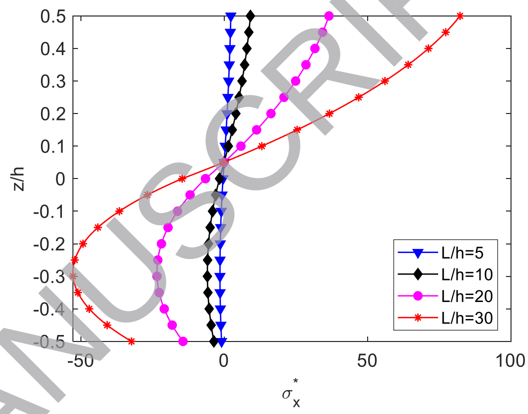

(b) $k = 1, \mu = 2$, (1-0-1) scheme

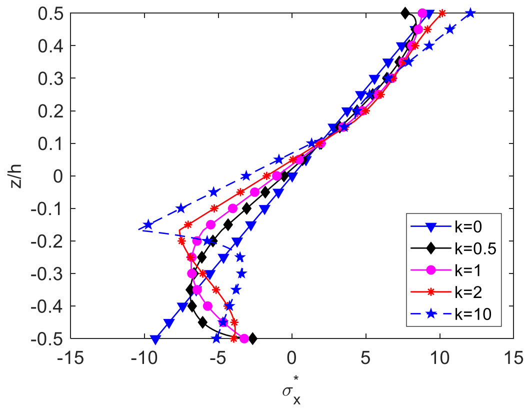

(c) $L/h = 10, \mu = 3$, (1-1-1) scheme

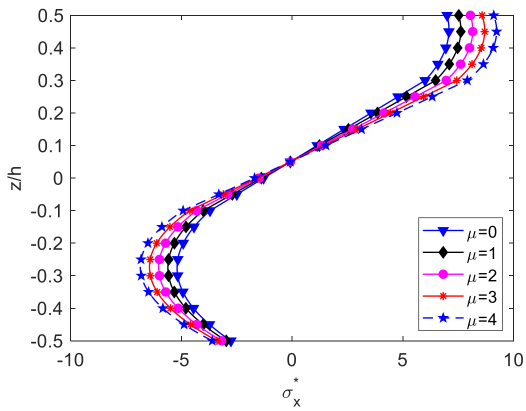

(d) $L/h = 10, k = 1$, (2-2-1) scheme

Fig. 4 The distribution of the normal stress through the thickness of the bi-FGSW nanobeams

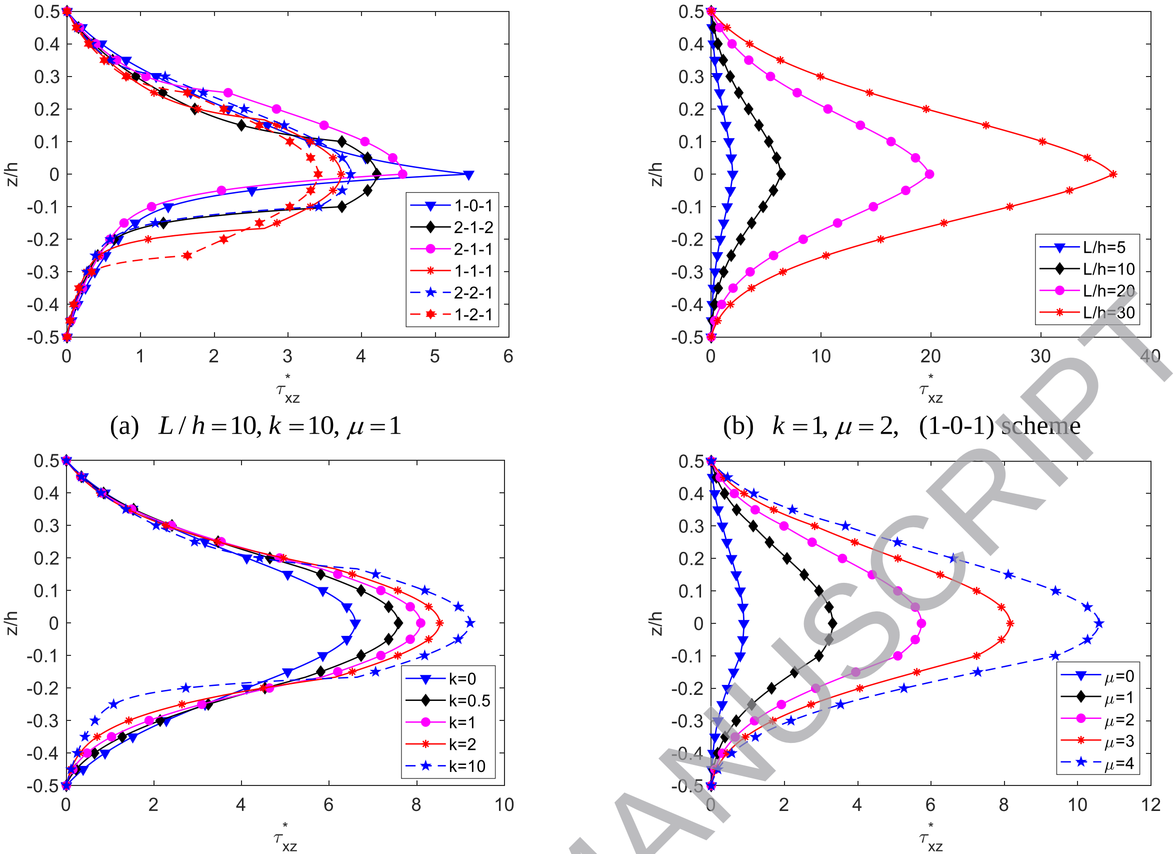

(a) $L/h=10,\ k=10,\ \mu=1$ (b) $k=1,\ \mu=2$, (1-0-1) scheme

(c) $L/h=10,\ \mu=3$, (1-1-1) scheme (d) $L/h=10,\ k=1$, (2-2-1) scheme

Fig. 5 The distribution of the transverse shear stress through the thickness of the bi-FGSW nanobeams

Table 12 The dimensionless first six frequencies of the bi-FGSW nanobeams ($L/h=10$)

Scheme	k	$\mu(\mathrm{nm}^2)$	Mode					
			(1)	(2)	(3)	(4)	(5)	(6)
1-0-1	0	0	12.0030	45.8894	96.7550	159.4610	229.9964	305.6285
		2	10.9691	34.3034	58.0660	78.1984	94.4100	107.3464
		4	10.1633	28.5742	45.3442	58.9524	69.7612	78.3605
	1	0	7.2770	28.0656	59.8499	99.7958	145.5022	195.1951
		2	6.6502	20.9797	35.9180	48.9391	59.7264	68.5587
		4	6.1617	17.4758	28.0486	36.8943	44.1329	50.0464
	10	0	5.1965	20.0932	43.0002	71.9804	105.3601	141.8796
		2	4.7489	15.0202	25.8059	35.2986	43.2487	49.8326
		4	4.4000	12.5116	20.1520	26.6110	31.9572	36.3767
2-2-1	0.5	0	9.5949	36.8500	78.1504	129.5616	187.8768	250.8134
		2	8.7684	27.5463	46.9008	63.5360	77.1205	88.0936
		4	8.1243	22.9457	36.6252	47.8986	56.9857	64.3064
	1	0	8.5053	32.7526	69.7021	115.9711	168.7314	225.9198
		2	7.7727	24.4834	41.8307	56.8713	69.2616	79.3502
		4	7.2017	20.3943	32.6659	42.8743	51.1787	57.9239
	10	0	6.3882	24.7469	53.0905	89.1042	130.7478	176.4554
		2	5.8379	18.4989	31.8615	43.6960	53.6699	61.9767
		4	5.4091	15.4093	24.8809	32.9416	39.6577	45.2416

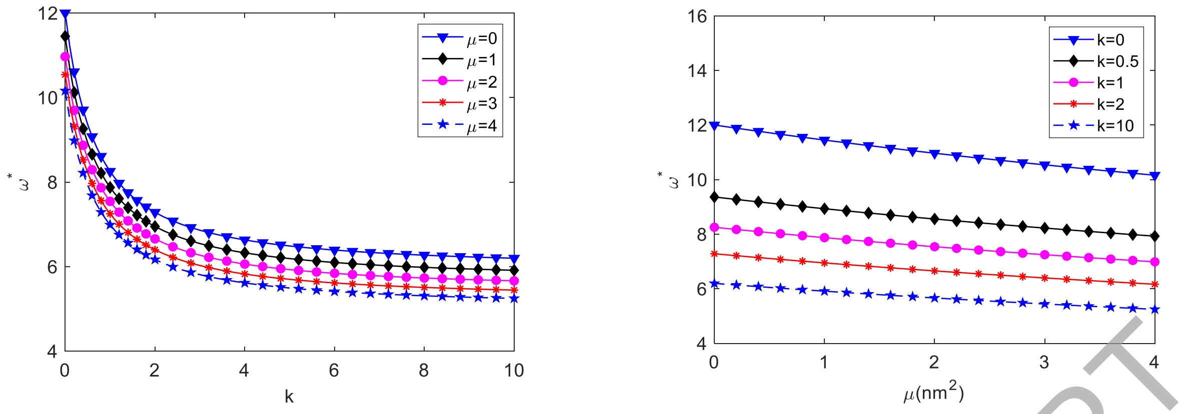

(a) (b)

Fig. 6 The variation of the dimensionless fundamental frequencies of the (1-1-1) bi-FGSW nanobeams with L/h = 10

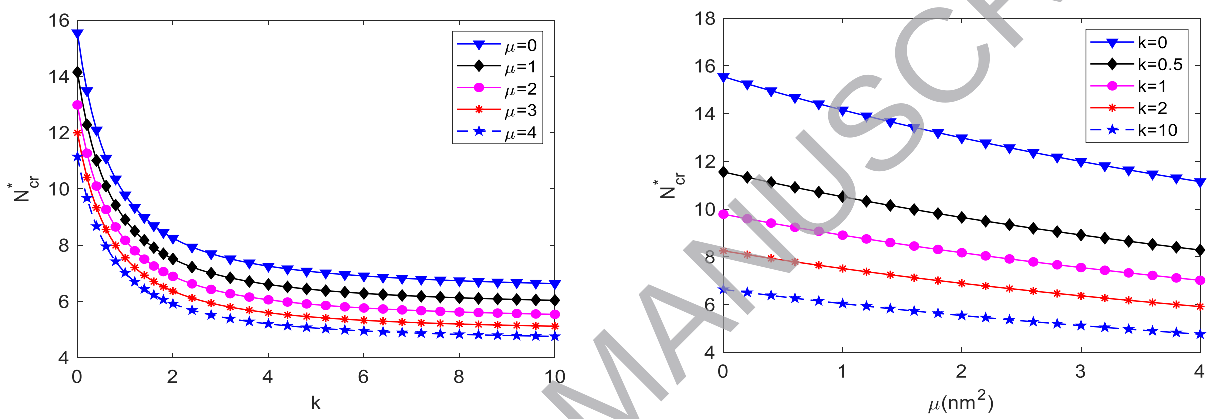

(a) (b)

Fig. 7 The variation of the dimensionless critical buckling load of the (1-1-1) bi-FGSW nanobeams with L/h = 10

Table 13 The dimensionless critical buckling load N_{cr}^{*} of the bi-FGSW nanobeams

L/h	k	$\mu(\mathrm{nm}^2)$	1-0-1	2-1-2	2-1-1	1-1-1	2-2-1	1-2-1
5	0	0	115.7952	115.7952	115.7952	115.7952	115.7952	115.7952
		1	105.3933	105.3933	105.3933	105.3933	105.3933	105.3933
		2	96.7062	96.7062	96.7062	96.7062	96.7062	96.7062
		3	89.3421	89.3421	89.3421	89.3421	89.3421	89.3421
		4	83.0202	83.0202	83.0202	83.0202	83.0202	83.0202
	1	0	64.9717	69.9929	68.0249	74.3476	73.4773	81.2766
		1	59.1352	63.7055	61.9142	67.6690	66.8768	73.9755
		2	54.2610	58.4545	56.8109	62.0913	61.3645	67.8780
		3	50.1290	54.0032	52.4848	57.3631	56.6916	62.7092
		4	46.5819	50.1819	48.7709	53.3040	52.6801	58.2718
	10	0	42.1462	46.5922	43.3909	51.0635	48.6194	59.5729
		1	38.3602	42.4068	39.4931	46.4765	44.2519	54.2214
		2	35.1984	38.9114	36.2378	42.6456	40.6044	49.7522
		3	32.5180	35.9483	33.4784	39.3982	37.5124	45.9636
		4	30.2170	33.4046	31.1094	36.6104	34.8580	42.7112
10	0	0	15.5455	15.5455	15.5455	15.5455	15.5455	15.5455
		1	14.1490	14.1490	14.1490	14.1490	14.1490	14.1490

Table 13 Continued

L/*h*	*k*	μ(nm^2)	1-0-1	2-1-2	2-1-1	1-1-1	2-2-1	1-2-1
	0	2	12.9828	12.9828	12.9828	12.9828	12.9828	12.9828
		3	11.9941	11.9941	11.9941	11.9941	11.9941	11.9941
		4	11.1454	11.1454	11.1454	11.1454	11.1454	11.1454
	1	0	8.5373	9.1969	8.9392	9.7835	9.6680	10.7318
		1	7.7704	8.3707	8.1362	8.9046	8.7995	9.7678
		2	7.1299	7.6808	7.4656	8.1706	8.0742	8.9627
10		3	6.5870	7.0959	6.8971	7.5484	7.4594	8.2802
		4	6.1209	6.5938	6.4090	7.0143	6.9315	7.6943
	10	0	5.5236	6.0536	5.6437	6.6324	6.3099	7.7688
		1	5.0274	5.5098	5.1368	6.0366	5.7431	7.0709
		2	4.6130	5.0556	4.7134	5.5391	5.2697	6.4881
		3	4.2617	4.6707	4.3544	5.1173	4.8684	5.9940
		4	3.9602	4.3402	4.0463	4.7552	4.5239	5.5699

nanobeams are presented in Table 12. It can see clearly that the frequencies of the bi-FGSW nanobeams decrease as the growth of the slender ratio, the power-law index as well as the nonlocal parameter. The effects the power-law index and nonlocal parameters on the dimensionless fundamental frequency of the bi-FGSW nanobeams are present in Fig. 6. In which the slender ratio of the beam is $L/h = 10$. It is obvious that when the power-law index rises, the frequency of the bi-FGSW nanobeams decreases at a high speed if $k \in [0,2]$, and it decreases at a lower speed if $k > 2$. The inclusion of the nonlocal parameter leads to the decrease of the frequency of the bi-FGSW nanobeams as presented in Fig. 6(b).

3.2.3 Buckling analysis of bi-FGSW nanobeams

The buckling behavior of the simply supported bi-FGSW nanobeams is investigated in this subsection. Table 13 gives the dimensionless critical buckling load of the bi-FGSW nanobeams with different values of the slender ratio, the power-law index and the nonlocal parameter. According to this table, the slender ratio has strong effects on the buckling behavior of the bi-FGSW nanobeams. When the slender ratio, the power-law index and the nonlocal parameter increase, the critical buckling load of the bi-FGSW nanobeams decreases. Fig. 7 demonstrates the influence of the power-law index and the nonlocal parameters on the critical buckling load of the bi-FGSW nanobeams with the slender ratio of $L/h = 10$. According to Fig. 7, the critical buckling load is decreased when the power-law index *k* increase. Besides, the critical buckling load decreases when the nonlocal parameter is included in the computation.

5. Conclusions

A refined simple shear deformation theory in combination with nonlocal elastic theory has been established in this work to analyze the bending, free vibration and buckling of novel bi-functionally graded sandwich nanobeams. The proposed theory takes into account the transverse shear strain and stress through the thickness of the beam without demanding a shear correction factor. The comparison study has shown that the proposed theory is accuracy and efficiency in calculating the deflections, stresses, free vibration and buckling behavior of the nanobeams. According to the numerical results of the parameter study, some following remarkable points can be presented as

• The bending, free vibration and buckling behavior of the bi-FGSW nanobeams are completely different to usual ones, especially the distribution of the stresses through the thickness direction.

• The use of bi-FGSW nanobeams can avoid the phenomenon of the stress concentration at the top and bottom surfaces of the beams.

• The small-scale effects play a considerable role on the mechanical behavior of the bi-FGSW nanobeams. The inclusion of the nonlocal parameter leads to an increase in the deflection of bi-FGSW nanobeams. On the other hand, the inclusion of the small-scale effects leads to a reduction of the natural frequencies and critical buckling loads of bi-FGSW nanobeams.

The results of this study can serve as benchmarks for the future works on the bending, free vibration and buckling response of the bi-FGSW beams, plates and shells which may have a huge potential application in engineering and industry.

References

Ahmed, H.M.S., Aicha, B., Fabrice, B., Abdelouahed, T. and Samy, R.M. (2018), “Buckling analysis of new quasi-3D FG nanobeams based on nonlocal strain gradient elasticity theory and variable length scale parameter”, *Steel Compos. Struct.*, **28**(1), 13-24. https://doi.org/10.12989/SCS.2018.28.1.013.

Apetre, N.A., Sankar, B.V. and Ambur, D.R. (2008), “Analytical modeling of sandwich beams with functionally graded core”, *J.*

Sandw. *Struct*. *Mater*., **10**(1), 53-74. https://doi.org/10.1177/1099636207081111.

Arefi, M. and Zenkour, A.M. (2016), "A simplified shear and normal deformations nonlocal theory for bending of functionally graded piezomagnetic sandwich nanobeams in magneto-thermo-electric environment", *J*. *Sandw*. *Struct*. *Mater*., **18**(5), 624-651. https://doi.org/10.1177/1099636216652581.

Aria, A.I. and Friswell, M.I. (2019), "A nonlocal finite element model for buckling and vibration of functionally graded nanobeams", *Compos*. *Part B Eng*., **166**, 233-246. https://doi.org/10.1016/j.compositesb.2018.11.071.

Aria, A.I., Rabczuk, T. and Friswell, M.I. (2019), "A finite element model for the thermo-elastic analysis of functionally graded porous nanobeams", *Eur*. *J*. *Mech*. *A Solid*, **77**, 103767. https://doi.org/10.1016/j.euromechsol.2019.04.002.

Bakoura, A., Bourada, F., Bousahla, A.A., Tounsi, A., Benrahou, K.H, Tounsi, A, Al-Zahrani, M.M. and Mahmoud, S.R. (2021), "Buckling analysis of functionally graded plates using HSDT in conjunction with the stress function method", *Comput*. *Concrete*, **27**(1), 73-83. http://dx.doi.org/10.12989/cac.2021.27.1.073.

Balubaid, M., Tounsi, A., Dakhel, B. and Mahmoud, S.R. (2019), "Free vibration investigation of FG nanoscale plate using nonlocal two variables integral refined plate theory", *Comput*. *Concrete*, **24**(6), 579-586. https://doi.org/10.12989/CAC.2019.24.6.579

Bellal, M., Hebali, H., Heireche, H., Bousahla, A.A., Tounsi, A., Bourada, F., Mahmoud, S.R., Bedia, E.A.A. and Tounsi, A. (2020), "Buckling behavior of a single-layered graphene sheet resting on viscoelastic medium via nonlocal four-unknown integral model", *Steel Compos*. *Struct*., **34**(5), 643-655. https://doi.org/10.12989/SCS.2020.34.5.643,

Bellifa, H., Benrahou, K.H., Bousahla, A.A., Tounsi, A. and Mahmoud, S.R. (2017), "A nonlocal zeroth-order shear deformation theory for nonlinear postbuckling of nanobeams", *Struct*. *Eng*. *Mech*., **62**(6), 695-702. https://doi.org/10.12989/SEM.2017.62.6.695.

Bensaid, I., Daikh, A.A. and Drai, A. (2020), "Size-dependent free vibration and buckling analysis of sigmoid and power law functionally graded sandwich nanobeams with microstructural defects", *Proceedings of the Institution of Mechanical Engineers*, *Part C: Journal of Mechanical Engineering Science*, **234**(18), 3667-3688.

Berghouti, H., Adda Bedia, E.A., Benkhedda, A. and Tounsi, A. (2019), "Vibration analysis of nonlocal porous nanobeams made of functionally graded material", *Adv*. *Nano Res*., **7**(5), 351-364. https://doi.org/10.12989/ANR.2019.7.5.351.

Bouafia, K., Kaci, A., Houari, M.S.A., Benzair, A. and Tounsi, A. (2017), "A nonlocal quasi-3D theory for bending and free flexural vibration behaviors of functionally graded nanobeams", *Smart Struct*. *Syst*., **19**(2), 115-126. https://doi.org/10.12989/SSS.2017.19.2.115.

Boussoula, A., Boucham, B., Bourada, M., Bourada, F., Tounsi, A., Bousahla, A.A. and Tounsi, A. (2020), "A simple nth-order shear deformation theory for thermomechanical bending analysis of different configurations of FG sandwich plates", *Smart Struct*. *Syst*., **25**(2), 197-218. https://doi.org/10.12989/SSS.2020.25.2.197.

Boutaleb, S., Benrahou, K.H., Bakora, A., Algarni, A., Bousahla, A.A,. Tounsi, A. and Tounsi, A. (2019), "Dynamic analysis of nanosize FG rectangular plates based on simple nonlocal quasi 3D HSDT", *Adv*. *Nano Res*., **7**(3), 191-208. https://doi.org/10.12989/ANR.2019.7.3.191.

Chikr, S.C., Kaci, A., Bousahla, A.A., Bourada, F., Tounsi, A., Bedia, E.A.A., Mahmoud, S.R., Benrahou, K.H. and Tounsi, A. (2020), "A novel four-unknown integral model for buckling response of FG sandwich plates resting on elastic foundations under various boundary conditions using Galerkin's approach", *Geomech*. *Eng*., **21**(5), 471-487. https://doi.org/10.12989/GAE.2020.21.5.471.

Eringen, A.C. (1983), "On differential equations of nonlocal elasticity and solutions of screw dislocation and surface waves", *J*. *Appl*. *Phys*., **54**, 4703-4710. https://doi.org/10.1063/1.332803.

Hadj, B., Rabia, B. and Daouadji, T.H. (2019), "Influence of the distribution shape of porosity on the bending FGM new plate model resting on elastic foundations", *Struct*. *Eng*. *Mech*., **72**(1), 61-70. https://doi.org/10.12989/SEM.2019.72.1.061.

Hamed, M.A., Eltaher, M.A., Sadoun, A.M. and Almitani, K.H. (2016), "Free vibration of symmetric and sigmoid functionally graded nanobeams", *Appl*. *Phys*. *A*, **122**(9), 829. https://doi.org/10.1007/s00339-016-0324-0.

Hana, B., Adda Bedia, E.A., Amina, B. and Abdelouahed, T. (2019), "Vibration analysis of nonlocal porous nanobeams made of functionally graded material", *Adv*. *Nano Res*., **7**(5), 351-364. https://doi.org/10.12989/ANR.2019.7.5.351.

Hussain, M., Naeem, M.N., Tounsi, A. and Taj, M. (2019), "Nonlocal effect on the vibration of armchair and zigzag SWCNTs with bending rigidity", *Adv*. *Nano Res*., **7**(6), 431-442. https://doi.org/10.12989/ANR.2019.7.6.431.

Karamanlı, A. (2017), "Bending behaviour of two directional functionally graded sandwich beams by using a quasi-3d shear deformation theory", *Compos*. *Struct*., **174**, 70-86. https://doi.org/10.1016/j.compstruct.2017.04.046.

Larbi, C.F., Abdelhakim, K., Ahmed, H.M.S., Abdelouahed, T., Anwar, B.O. and Samy, R.M. (2015), "Bending and buckling analyses of functionally graded material (FGM) size-dependent nanoscale beams including the thickness stretching effect", *Steel Compos*. *Struct*., **18**(2), 425-442. https://doi.org/10.12989/SCS.2015.18.2.425.

Li, W., Ma, H. and Gao, W. (2019), "A higher-order shear deformable mixed beam element model for accurate analysis of functionally graded sandwich beams", *Compos*. *Struct*., **221**, 110830. https://doi.org/10.1016/j.compstruct.2019.04.002.

Liu, H., Lv, Z. and Wu, H. (2019), "Nonlinear free vibration of geometrically imperfect functionally graded sandwich nanobeams based on nonlocal strain gradient theory" *Compos*. *Struct*., **214**, 47-61. https://doi.org/10.1016/j.compstruct.2019.01.090.

Mama, A., Ahmed, H.M.S., Adda, B.E.A. and Abdelouahed, T. (2016), "Size-dependent mechanical behavior of functionally graded trigonometric shear deformable nanobeams including neutral surface position concept", *Steel Compos*. *Struct*., **20**(5), 963-981. https://doi.org/10.12989/SCS.2016.20.5.963.

Matouk, H., Bousahla, A.A., Heireche, H., Bourada, F., Bedia, E.A.A., Tounsi, A., Mahmoud, S.R., Tounsi, A. and Benrahou, K.H. (2020), "Investigation on hygro-thermal vibration of P-FG and symmetric S-FG nanobeam using integral Timoshenko beam theory", *Adv*. *Nano Res*., **8**(4), 293-305. https://doi.org/10.12989/ANR.2020.8.4.293.

Menasria, A., Kaci, A., Bousahla, A.A., Bourada, F., Tounsi, A., Benrahou, K.H., Tounsi, A., Adda Bedia, E.A. and Mahmoud, S.R. (2020), "A four-unknown refined plate theory for dynamic analysis of FG-sandwich plates under various boundary conditions", *Steel Compos*. *Struct*., **36**(3), 355-367. https://doi.org/10.12989/SCS.2020.36.3.355.

Nguyen, T.K. and Nguyen, B.D. (2015), "A new higher-order shear deformation theory for static, buckling and free vibration analysis of functionally graded sandwich beams", *J*. *Sandw*. *Struct*. *Mater*., **17**(6), 613-631. https://doi.org/10.1177/1099636215589237.

Nguyen, T.K., Truong-Phong Nguyen, T., Vo, T.P. and Thai, H.T. (2015), "Vibration and buckling analysis of functionally graded sandwich beams by a new higher-order shear deformation theory", *Compos*. *Part B Eng*., **76**, 273-285. https://doi.org/10.1016/j.compositesb.2015.02.032.

Nguyen, T.K., Vo, T.P., Nguyen, B.D. and Lee, J. (2016), "An analytical solution for buckling and vibration analysis of functionally graded sandwich beams using a quasi-3D shear deformation theory", *Compos*. *Struct*., **156**, 238-252. https://doi.org/10.1016/j.compstruct.2015.11.074.

Gao, X.L. and Zhang, G.Y., (2015), "A microstructure- and surface energy-dependent third-order shear deformation beam model", *J*. *Appl*. *Math*. *Phys*., **66**, 1871-1894. https://doi.org/10.1007/s00033-014-0455-0.

Osofero, A.I., Vo, T.P., Nguyen, T.K. and Lee, J. (2015), "Analytical solution for vibration and buckling of functionally graded sandwich beams using various quasi-3D theories", *J*. *Sandw*. *Struct*. *Mater*., **18**(1), 3-29. https://doi.org/10.1177/1099636215582217.

Rabhi, M., Benrahou, K.H., Kaci, A., Houari, M.S.A., Bourada, F., Bousahla, A.A., Tounsi, A., Adda Bedia, E.A. Mahmoud, S.R. and Tounsi, A. (2020), "A new innovative 3-unknowns HSDT for buckling and free vibration of exponentially graded sandwich plates resting on elastic foundations under various boundary conditions", *Geomech*. *Eng*., **22**(2), 119-132. https://doi.org/10.12989/GAE.2020.22.2.119.

Riadh, B., Ait, A.H. and Abdelouahed, T. (2015), "A new higher-order shear and normal deformation theory for functionally graded sandwich beams", *Steel Compos*. *Struct*., **19**(3), 521-546. https://doi.org/10.12989/SCS.2015.19.3.521.

Şimşek, M. (2019), "Some closed-form solutions for static, buckling, free and forced vibration of functionally graded (FG) nanobeams using nonlocal strain gradient theory", *Compos*. *Struct*., **224**, 111041. https://doi.org/10.1016/j.compstruct.2019.111041.

Şimşek, M. and Al-shujairi, M. (2017), "Static, free and forced vibration of functionally graded (FG) sandwich beams excited by two successive moving harmonic loads", *Compos*. *Part B Eng*., **108**, 18-34. https://doi.org/10.1016/j.compositesb.2016.09.098.

Songsuwan, W., Pimsarn, M. and Wattanasakulpong, N. (2018), "Dynamic responses of functionally graded sandwich beams resting on elastic foundation under harmonic moving loads", *Int*. *J*. *Struct*. *Stabil*. *Dyn*., **18**(09), 1850112. https://doi.org/10.1142/S0219455418501122.

Thai, H.T. and Vo, T.P. (2012), "A nonlocal sinusoidal shear deformation beam theory with application to bending, buckling, and vibration of nanobeams", *Int*. *J*. *Eng*. *Sci*., **54**, 58-66. https://doi.org/10.1016/j.ijengsci.2012.01.009.

Tossapanon, P. and Wattanasakulpong, N. (2016), "Stability and free vibration of functionally graded sandwich beams resting on two-parameter elastic foundation", *Compos*. *Struct*., **142**, 215-225. https://doi.org/10.1016/j.compstruct.2016.01.085.

Trinh, L.C., Vo, T.P., Osofero, A.I. and Lee, J. (2016), "Fundamental frequency analysis of functionally graded sandwich beams based on the state space approach", *Compos*. *Struct*., **156**, 263-275. https://doi.org/10.1016/j.compstruct.2015.11.010.

Vinh, P.V. (2021), "Deflections, stresses and free vibration analysis of bi-functionally graded sandwich plates resting on Pasternak's elastic foundations via a hybrid quasi-3D theory", *Mech*. *Based Des*. *Struct*., **1**, 1-32. https://doi.org/10.1080/15397734.2021.1894948.

Vo, T.P., Thai, H.T., Nguyen, T.K., Maheri, A. and Lee, J. (2014), "Finite element model for vibration and buckling of functionally graded sandwich beams based on a refined shear deformation theory", *Eng*. *Struct*., **64**, 12-22. https://doi.org/10.1016/j.engstruct.2014.01.029.

Vo, T.P., Thai, H.T., Nguyen, T.K., Inam, F. and Lee, J. (2015a), "A quasi-3D theory for vibration and buckling of functionally graded sandwich beams", *Compos*. *Struct*., **119**, 1-12. https://doi.org/10.1016/j.compstruct.2014.08.006.

Vo, T.P., Thai, H.T., Nguyen, T.K., Inam, F. and Lee, J. (2015b), "Static behaviour of functionally graded sandwich beams using a quasi-3D theory", *Compos*. *Part B Eng*., **68**, 59-74. https://doi.org/10.1016/j.compositesb.2014.08.030.

Yang, T., Tang, Y., Li, Q. and Yang, X.D. (2018), "Nonlinear bending, buckling and vibration of bi-directional functionally graded nanobeams", *Compos*. *Struct*., **204**, 313-319. https://doi.org/10.1016/j.compstruct.2018.07.045.

Yang, G., Wan Shen, X. and Haiping, Z. (2019), "Nonlinear thermal buckling of bi-directional functionally graded nanobeams", *Struct*. *Eng*. *Mech*., **71**(6), 669-682. https://doi.org/10.12989/SEM.2019.71.6.669.

Yarasca, J., Mantari, J.L. and Arciniega, R.A. (2016), "Hermite-Lagrangian finite element formulation to study functionally graded sandwich beams", *Compos*. *Struct*., **140**, 567-581. https://doi.org/10.1016/j.compstruct.2016.01.015.

Zhang, G.Y. and Gao, X.L., (2020), "A new Bernoulli-Euler beam model based on a reformulated strain gradient elasticity theory", *Math*. *Mech*. *Solids*, **25**, 630-643. https://doi.org/10.1177/1081286519886003.

Zemri, A., Houari, M.S.A., Bousahla, A.A. and Tounsi, A. (2015), "A mechanical response of functionally graded nanoscale beam: an assessment of a refined nonlocal shear deformation theory beam theory", *Struct*. *Eng*. *Mech*., **54**(4), 693-710. https://doi.org/10.12989/SEM.2015.54.4.693.

Zine, A, Bousahla, A.A., Bourada, F., Benrahou, K.H., Tounsi, A., Adda Bedia, E.A., Mahmoud, S.R. and Tounsi, A. (2020), "Bending analysis of functionally graded porous plates via a refined shear deformation theory", *Comput*. *Concrete*, **26**(1), 63-74. https://doi.org/10.12989/CAC.2020.26.1.063.

AT